Supporting Information

Photoinduced Intra-molecular Charge Transfer in an Electronically Modified Flavin Derivative: Roseoflavin

*Bora Karasulu and Walter Thiel**

Max-Planck-Institut für Kohlenforschung, Kaiser-Wilhelm-Platz 1, 45470, Mülheim, Germany

*Corresponding author: thiel@kofo.mpg.de

Contents

A. Assessing the performance of B3LYP and CAM-B3LYP for structural properties

B. Tables S1-S6: Structural properties: dihedral angles and bond lengths

C. Figures S1-S8: Frontier Kohn-Sham MOs; 3D representations of the energy surfaces of the LE and CT states with respect to dihedral angles; overlay of optimized geometries; DFT/MRCI dipole moments of the ground state and low-lying excited states

D. Choice of micro-solvation model

E. Color maps of energy contour plots

A. Assessing the performance of B3LYP and CAM-B3LYP for structural properties

For evaluating the performance of CAM-B3LYP[1] in comparison to conventional B3LYP, we optimized the ground state and the low-lying singlet and triplet excited states of RoLF in the gas phase using the 6-31G(d) basis set. The resulting pairs of dihedral angles (α / β) are collected in Table S1. Interestingly, WICT points could not be located on any singlet state surface with B3LYP, whereas those found with CAM-B3LYP correspond to saddle points.

In Table S1, one can identify the PICT, WICT, and TICT zwitterionic forms with the typical dihedral pairs (α/β) of about $21^o/-115^o$, $65^o/-65^o$, and $87^o/-87^o$, respectively, for both B3LYP and CAM-B3LYP, with some exceptions (like T1 and T2 with CAM-B3LYP). Evidently, the twist angles of the DMA group in the optimized GS, PICT, WICT, and TICT geometries from B3LYP and CAM-B3LYP only differ by up to $2\text{-}3^o$. For further comparisons, Table S2 lists the bond lengths in representative relaxed geometries of various types (GS, PICT, TICT, and T1) from either functional. Again, there are relatively small differences between B3LYP and CAM-B3LYP, which are largest for the T1 (planar) minimum geometries (average deviation of 0.016 Å) while the GS geometries are in very good agreement (average deviation of 0.006 Å). The Kohn-Sham MOs from B3LYP and CAM-B3LYP are generally also quite similar (Figure S1); in the PICT case, the HOMO-1 and HOMO-2 orbitals (n- and π-MOs) are very close in energy, and their order happens to be different in B3LYP and CAM-B3LYP. We consider the HOMO at the TICT minima (Figure S1) and focus on the bonds in TICT showing the largest deviation between B3LYP and CAM-B3LYP, namely C8-N8, C5a-N5, and C7-C6 (Table S2). Compared with B3LYP, CAM-B3LYP predicts shorter bonds, which can be attributed to the subtle enhanced bonding character of the HOMO between the corresponding atoms (Figure S1).

The dark-state crystal structure of roseoflavin in complex with a FMN riboswitch has been determined with a resolution of 3.0 Å (PDB id: 3F4H).[2] In this X-Ray structure, the DMA group is reported to assume a planar orientation with zero twist angle. This can arise from the presence of two conformers that are mirror images of each other with respect to the isoalloxazine plane. These two conformers have essentially equal energies and are thus populated equally. In such a case, crystallography will not differentiate between the two conformers and yield an average non-twisted planar geometry. Both the B3LYP and CAM-B3LYP calculations give two such mirror-image conformers for the ground state, in which the DMA group is slightly twisted because of the steric hindrance created by the neighboring methyl group (at the C7 position). The isoalloxazine ring adopts a planar conformation in the crystal structure, which is reproduced by both computational methods. The bond lengths from the crystal structure and their computed counterparts from B3LYP/PCM and CAM-B3LYP/PCM calculations are compiled in Table S3. The agreement between the experimental and theoretical results is equally good for both methods (average deviations of 0.024 Å and 0.025 Å, respectively).

B. Tables

Table S1. Dihedral angles (α and β, see Figure 2) for the DMA twist of the relaxed geometries obtained by gradient-following optimizations in the gas phase, at the B3LYP/6-31G(d) and CAM-B3LYP/6-31G(d) levels.

Gradients followed	B3LYP	CAM B3LYP
S0	19.6°/-119.6°	20.0°/-117.2°
S1	(a) 23.0°/-113.4° (b) 86.1°/-89.3° (c) 88.1°/-88.2° No WICT	(a) 22.4°/-114.5° (b) 20.1°/-116.9° (c) 65.3°/-65.2° (d) 87.0°/-87.0°
S2	(a) 23.0°/-113.4° No TICT or WICT	(a) 20.9°/-116.9° (b) 87.0°/-87.0° (c) 65.2°/-65.2°
S3	(a) 22.9°/-114.0° (b) 86.1°/-89.3° No WICT	(a) 23.6°/-111.0° (b) 20.6°/-117.2° (c) 65.2°/-65.1° No TICT
T1	(a) 20.6°/-122.4° (b) 65.3°/-65.1° No TICT	(a) 21.3°/-116.2° (bent)* (b) 20.8°/-121.8°(planar) No TICT or WICT.
T2	(a) 20.6°/-122.4° (b) 65.4°/-65.3° No TICT	(a) 37.8°/-96.9° (b) 65.4°/-65.4° No TICT.
T3	(a) 23.6°/-112.3° No TICT or WICT	(a) 24.1°/-110.5° (b) 65.2°/-65.2° No TICT.

* Each minimum geometry has a planar isoalloxazine moiety, except for T1 CAM-B3LYP.

Crossing of states was allowed during geometry optimizations at both levels of theory. As a consequence, the optimizations of higher-lying states generally ended up at the same stationary point on the lower-lying surface (as can be seen from very similar dihedral pairs).

Table S2. Bond lengths and related standard deviations (in Å) of selected minimum geometries computed at the B3LYP/6-31G(d) and CAM-B3LYP/6-31G(d) levels in the gas phase. The atom numbering is given in Figure 1.

Bond	GS minimum			PICT orientation			TICT orientation			T1 minimum (planar)		
	B3LYP	CAM-B3LYP	Abs. Diff.	B3LYP	CAM-B3LYP	Abs. Diff.	B3LYP	CAM-B3LYP	Abs. Diff.	B3LYP	CAM-B3LYP	Abs. Diff.
C10a - C4a	1.461	1.461	0.000	1.425	1.419	0.006	1.434	1.427	0.007	1.424	1.460	0.036
C10a - N10	1.388	1.377	0.011	1.379	1.391	0.012	1.409	1.398	0.011	1.399	1.362	0.037
C2 - O	1.217	1.210	0.007	1.226	1.215	0.011	1.225	1.217	0.008	1.224	1.207	0.017
C4 - N3	1.383	1.376	0.007	1.413	1.397	0.016	1.396	1.388	0.008	1.397	1.386	0.011
C4 - O	1.217	1.211	0.006	1.223	1.216	0.007	1.226	1.219	0.007	1.223	1.215	0.008
C4a - C4	1.497	1.494	0.003	1.458	1.461	0.003	1.471	1.466	0.005	1.470	1.465	0.005
C4a - N5	1.302	1.290	0.012	1.363	1.350	0.013	1.344	1.335	0.009	1.373	1.446	0.073
C5a - C6	1.410	1.404	0.006	1.414	1.408	0.006	1.411	1.427	0.016	1.423	1.417	0.006
C5a - N5	1.364	1.366	0.002	1.345	1.343	0.002	1.358	1.328	0.030	1.340	1.343	0.003
C7 - C6	1.381	1.375	0.006	1.390	1.380	0.010	1.395	1.370	0.025	1.380	1.381	0.001
C7 - R"	1.511	1.506	0.005	1.506	1.502	0.004	1.514	1.508	0.006	1.510	1.506	0.004
C8 - C7	1.435	1.427	0.008	1.437	1.436	0.001	1.396	1.414	0.018	1.439	1.416	0.023
C8 – N8	1.406	1.404	0.002	1.414	1.404	0.010	1.458	1.422	0.036	1.402	1.407	0.005
C9 - C8	1.403	1.394	0.009	1.399	1.391	0.008	1.404	1.417	0.013	1.410	1.419	0.009
C9a - C5a	1.420	1.408	0.012	1.446	1.447	0.001	1.431	1.435	0.004	1.451	1.440	0.011
C9a - C9	1.401	1.398	0.003	1.402	1.398	0.004	1.396	1.384	0.012	1.390	1.371	0.019
N1 - C10a	1.306	1.298	0.008	1.340	1.316	0.024	1.313	1.307	0.006	1.324	1.291	0.033
N1 - C2	1.384	1.381	0.003	1.398	1.396	0.002	1.382	1.377	0.005	1.391	1.401	0.010
N10 - C9a	1.387	1.385	0.002	1.391	1.374	0.017	1.390	1.381	0.009	1.393	1.429	0.036
N10 – R	1.466	1.460	0.006	1.467	1.458	0.009	1.454	1.450	0.004	1.459	1.451	0.008
N3 - C2	1.415	1.409	0.006	1.383	1.383	0.000	1.404	1.401	0.003	1.391	1.401	0.010
N8 - C_{Me1}	1.465	1.458	0.007	1.455	1.448	0.007	1.441	1.439	0.002	1.463	1.457	0.006
N8 - C_{Me2}	1.456	1.449	0.007	1.465	1.458	0.007	1.441	1.439	0.002	1.455	1.449	0.006
Average			0.006			0.008			0.011			0.016
Std. Dev.			0.003			0.006			0.009			0.017

Table S3. Comparison of experimental and computed bond lengths calculated at the B3LYP/6-31G(d) and CAM-B3LYP/6-31G(d) levels: GS minimum in water. The atom numbering is given in Figure 1.

Bond	Experimental[a]	B3LYP	Abs. Error	CAM-B3LYP	Abs. Error
C10a - C4a	1.398	1.437	0.027	1.448	0.035
C10a - N10	1.358	1.372	0.010	1.369	0.008
C2 - O	1.256	1.231	0.018	1.221	0.025
C4 - N3	1.357	1.371	0.010	1.371	0.010
C4 - O	1.256	1.225	0.022	1.218	0.027
C4a - C4	1.390	1.474	0.059	1.484	0.066
C4a - N5	1.351	1.313	0.026	1.300	0.036
C5a - C6	1.391	1.415	0.017	1.411	0.015
C5a - N5	1.349	1.338	0.008	1.353	0.003
C7 - C6	1.391	1.367	0.017	1.370	0.015
C7 - R"	1.507	1.509	0.001	1.507	0.000
C8 - C7	1.401	1.449	0.034	1.438	0.026
C8 – N8	1.367	1.365	0.001	1.388	0.014
C9 - C8	1.400	1.409	0.006	1.397	0.002
C9a - C5a	1.394	1.425	0.022	1.413	0.014
C9a - C9	1.395	1.387	0.005	1.395	0.000
N1 - C10a	1.364	1.321	0.031	1.312	0.037
N1 - C2	1.363	1.357	0.004	1.367	0.003
N10 - C9a	1.353	1.382	0.020	1.383	0.021
N10 – R	1.476	1.467	0.007	1.464	0.009
N3 - C2	1.357	1.400	0.031	1.406	0.034
N8 - C_{Me1}	1.454	1.457	0.002	1.452	0.001
N8 - C_{Me2}	1.451	1.463	0.009	1.461	0.007
Average			0.024		0.025
Std. Dev.			0.020		0.023

[a] The experimental values are taken from ref [2].

Table S4. Dihedral angles (α and β, see Figure 2) of the relaxed geometries obtained using various models and gradients at the (TD)CAM-B3LYP/6-31G(d) level. 'N/A': No unique relaxed geometry could be obtained for the given model by gradient following.

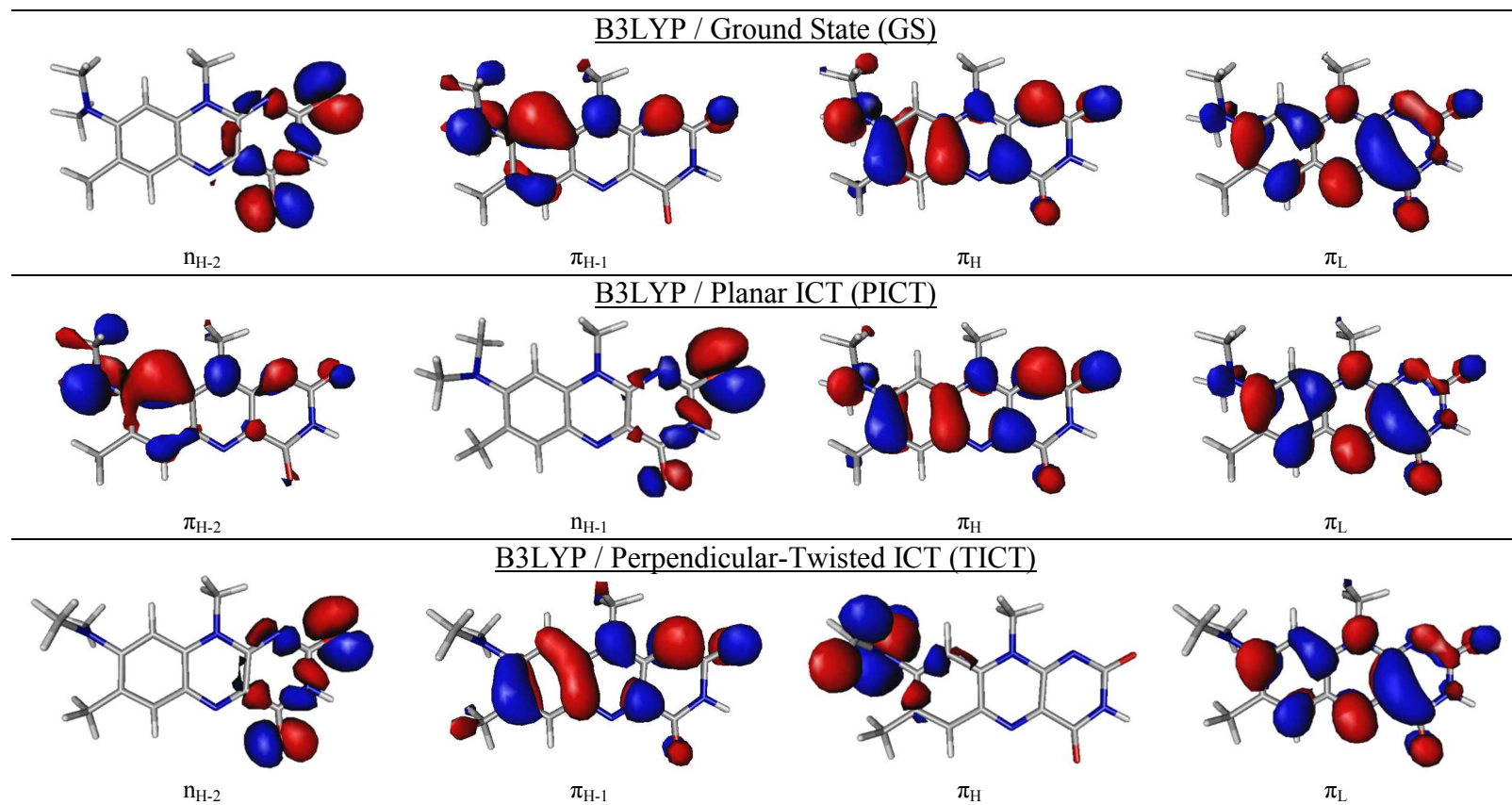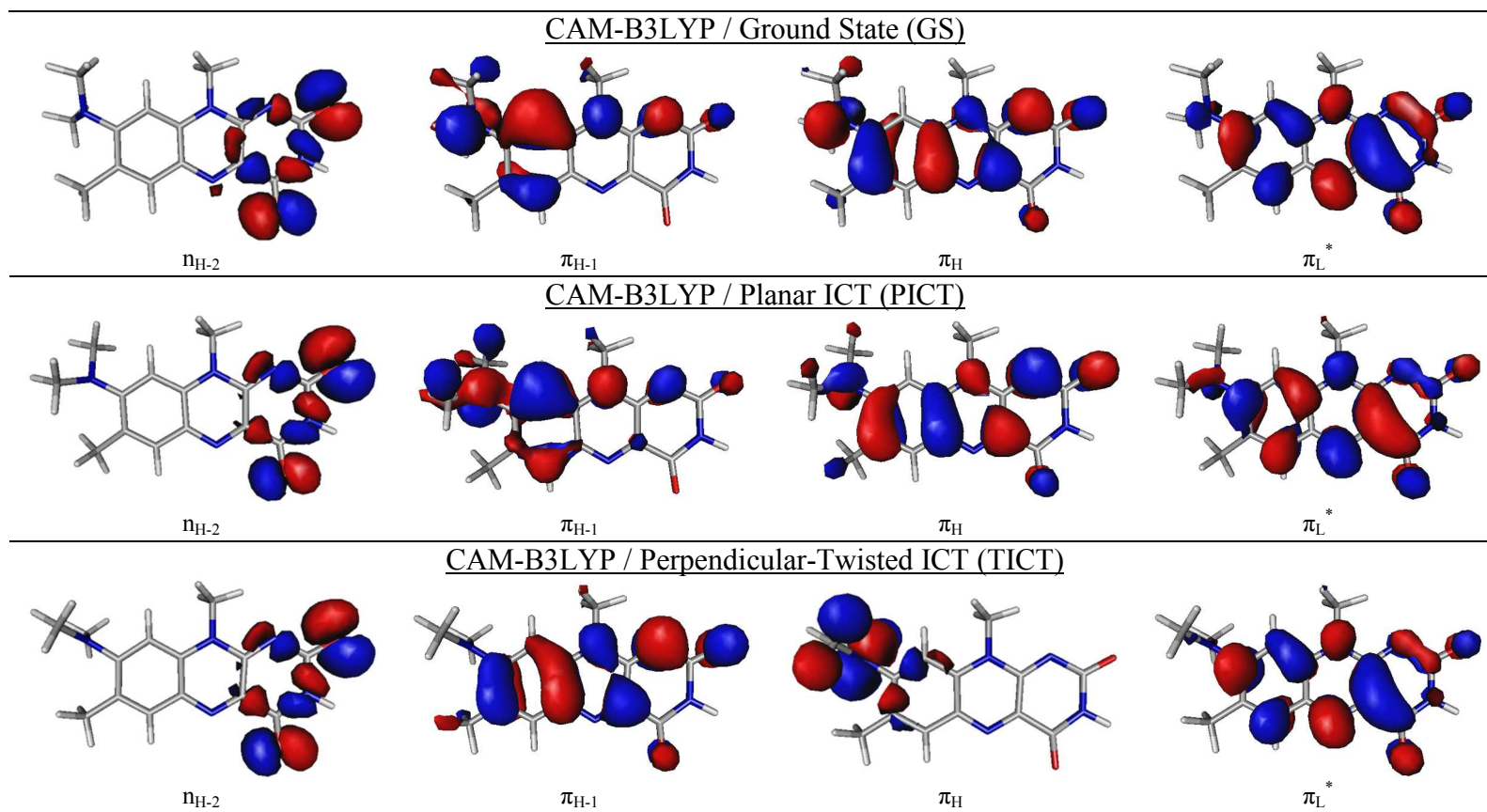| Gradients used	CAM- B3LYP Water		Water + Micro-solvation		CAM- B3LYP Benzene	
	Rotamer 1	Rotamer 2	Rotamer 1	Rotamer 2	Rotamer 1	Rotamer 2
S0	16.2° /-125.7°	N/A	15.6° / -133.7°	N/A	18.1° / -120.2°	N/A
S1	21.0° / -143.0° (PICT)	87.4° / -84.6 ° (TICT)	20.9° / -145.6° (PICT)	86.4° / -86.2 ° (TICT)	19.1° / -125.4° (PICT)	N/A °
S2	86.2° / -86.2° (TICT)	N/A	86.0° / -86.0° (TICT)	N/A	86.2 ° / -86.5° (TICT)	N/A
T1	20.3° / -148.5°	N/A	19.9° / -151.6°	N/A	-20.5° / -136.2°	N/A
T2	N/A		21.9° / -149.7°	N/A	-31.6°/ -104.3°	N/A

Table S5. Bond lengths and related standard deviations (in Å) in the GS, PICT, and TICT minima computed at the CAM-B3LYP/6-31G(d) level in the gas phase. The atom numbering is given in Figure 1.

Bond Name	Type of the Minimum Geometry			
	GS	PICT	TICT	std dev
C4a-N5	1.290	1.350	1.335	0.025
C4a-C10a	1.461	1.419	1.427	0.018
C9a-C5a	1.408	1.447	1.435	0.016
C5a-N5	1.366	1.343	1.328	0.015
C4-C4a	1.494	1.461	1.466	0.015
C4-O	1.211	1.216	1.219	0.003
C2-O	1.210	1.215	1.217	0.003
C7-C_{Me}	1.506	1.502	1.508	0.002

Table S6. Bond lengths and related standard deviations (in Å) in the GS, PICT, and TICT minima computed at the CAM-B3LYP/6-31G(d) level in water. The atom numbering is given in Figure 1.

Bond Name	Type of the Minimum Geometry			
	GS	PICT	TICT	std dev
C4a-N5	1.300	1.346	1.354	0.024
C8-N8	1.388	1.366	1.409	0.018
C5a-N5	1.353	1.353	1.319	0.016
C4a-C10a	1.448	1.426	1.413	0.015
C4-C4a	1.484	1.464	1.451	0.014
N8-C_{Mel}	1.452	1.452	1.444	0.004
C9a-N10	1.383	1.388	1.384	0.002
C7-C_{Me}	1.507	1.505	1.505	0.001

C. Figures

B3LYP / Ground State (GS)			
n_{H-2}	π_{H-1}	π_H	π_L

B3LYP / Planar ICT (PICT)			
π_{H-2}	n_{H-1}	π_H	π_L

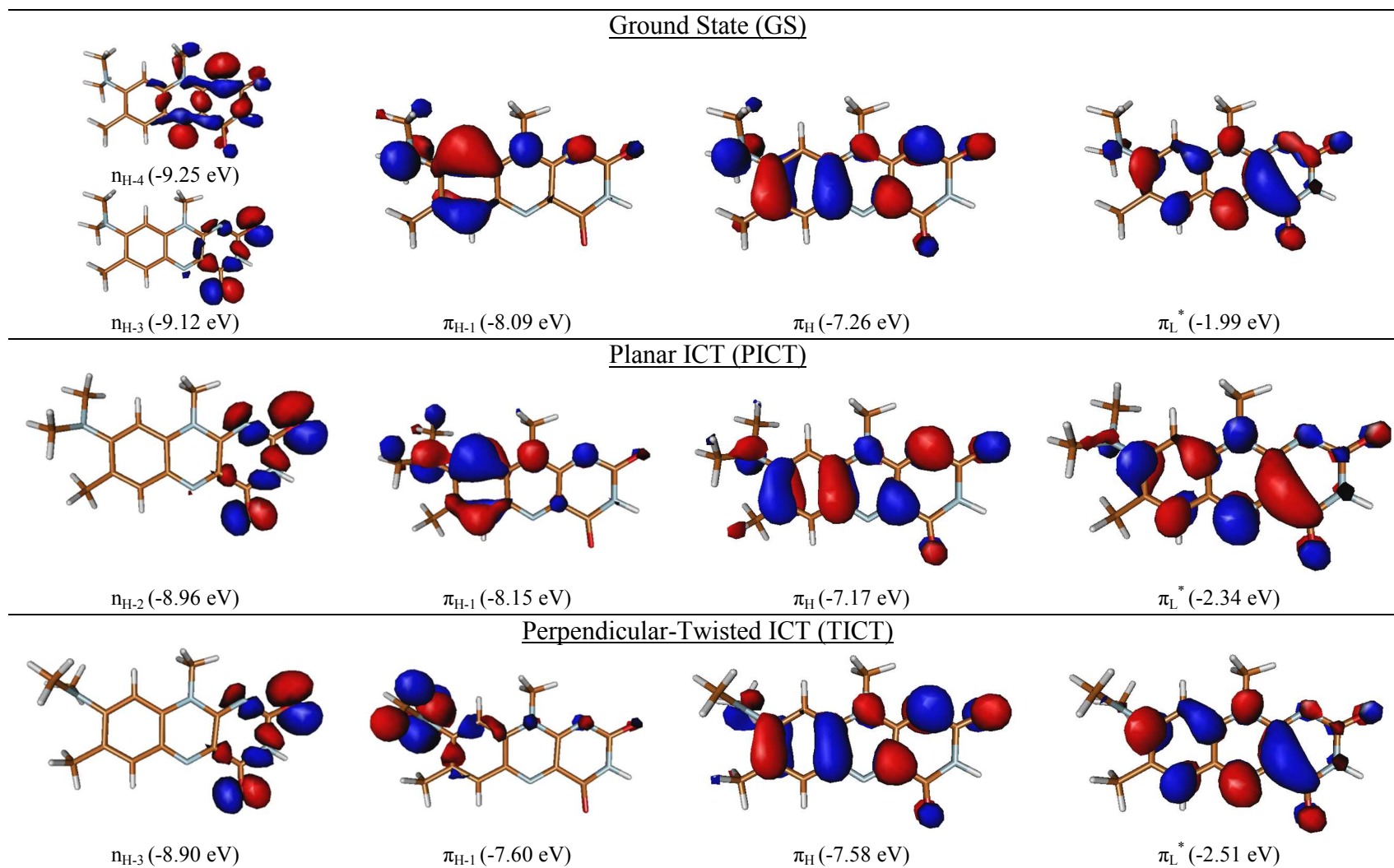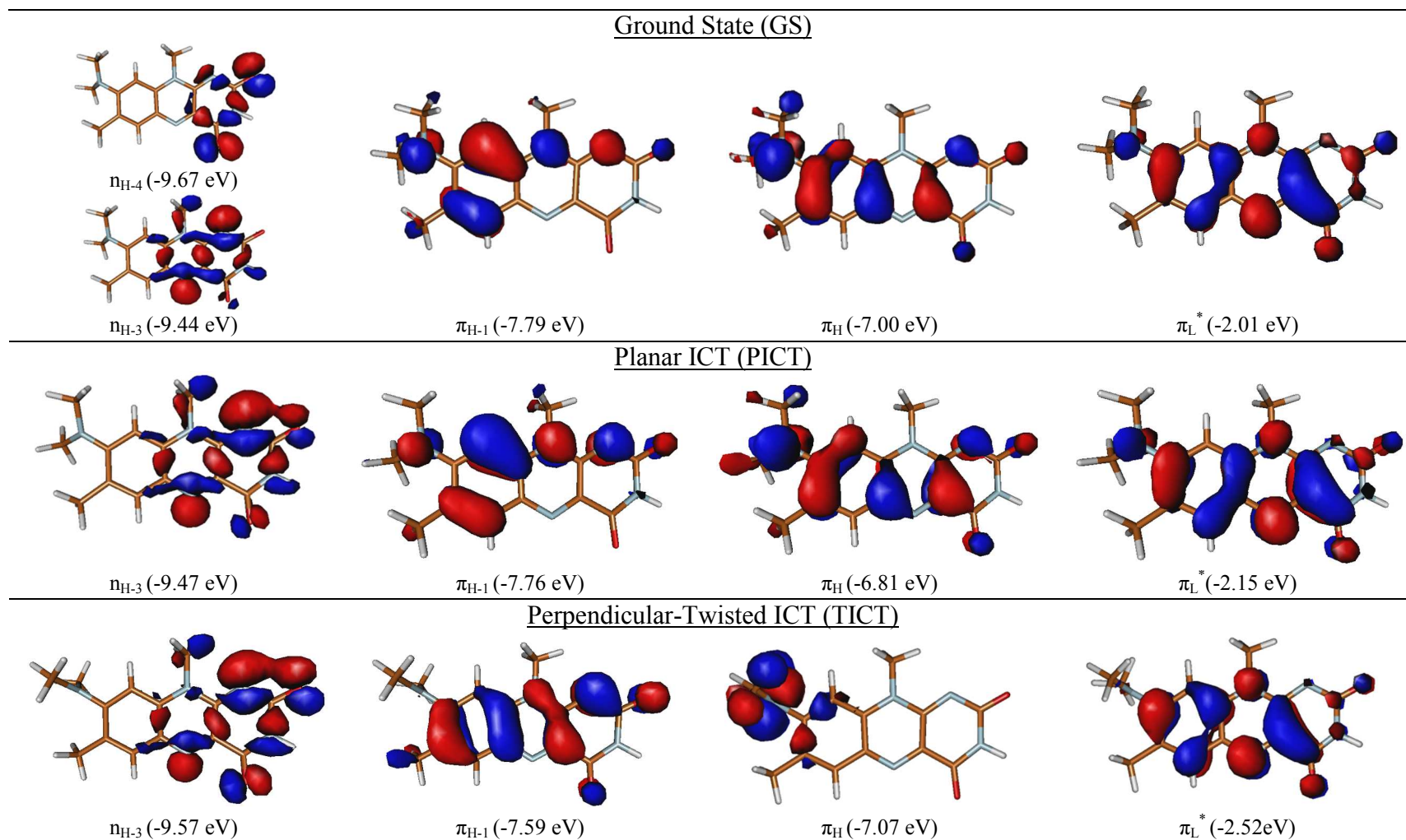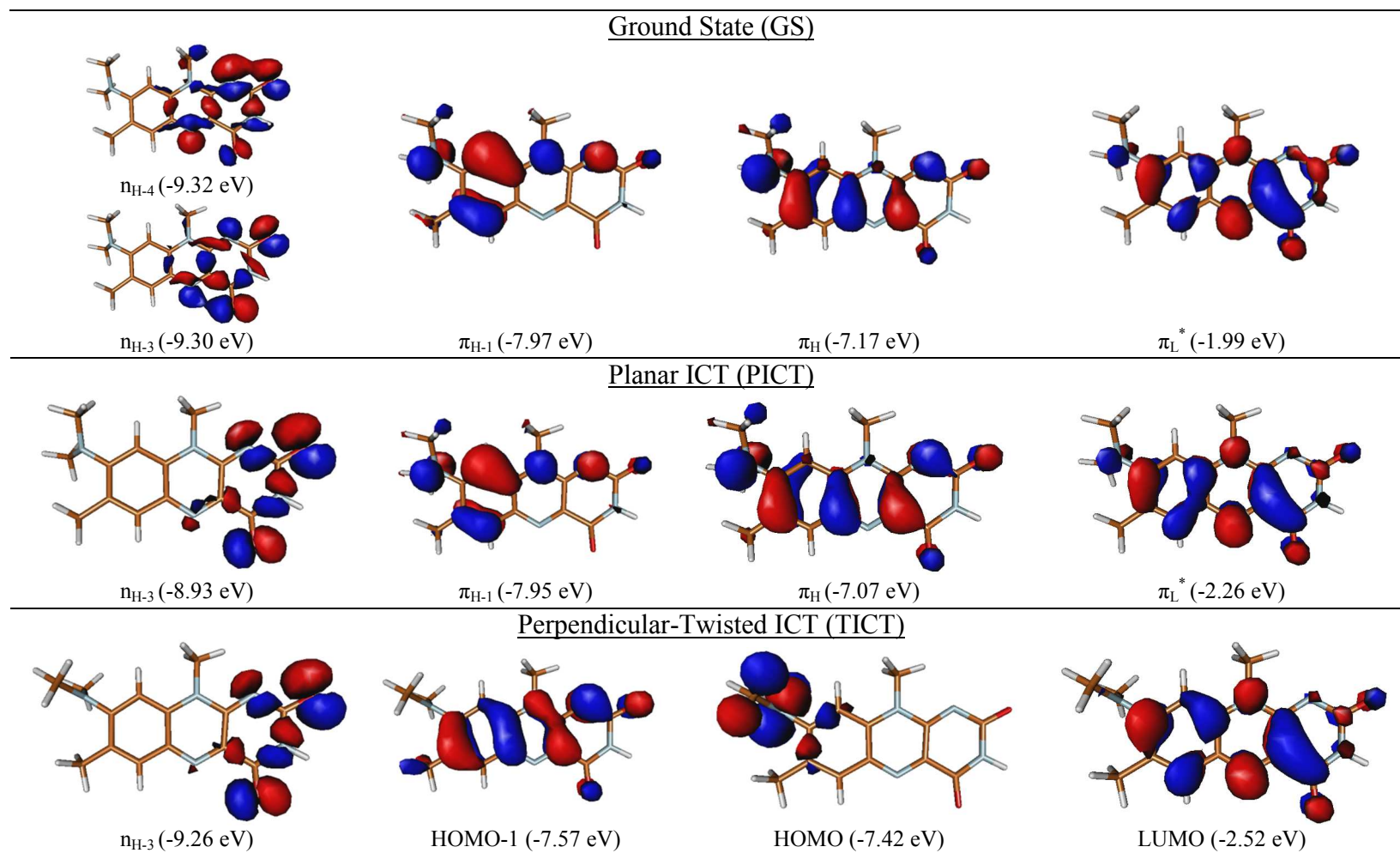| B3LYP / Perpendicular-Twisted ICT (TICT)			
n_{H-2}	π_{H-1}	π_H	π_L

Figure S1. The frontier Kohn-Sham orbitals computed at the GS, PICT, and TICT minima using B3LYP/6-31G(d) or CAM-B3LYP/6-31G(d) in the gas phase; visualized with MOLDEN using a contour value of 0.03.

Ground State (GS)

n$_{H-4}$ (-9.25 eV)

n$_{H-3}$ (-9.12 eV)   π$_{H-1}$ (-8.09 eV)   π$_H$ (-7.26 eV)   π$_L^*$ (-1.99 eV)

Planar ICT (PICT)

n$_{H-2}$ (-8.96 eV)   π$_{H-1}$ (-8.15 eV)   π$_H$ (-7.17 eV)   π$_L^*$ (-2.34 eV)

Perpendicular-Twisted ICT (TICT)

n$_{H-3}$ (-8.90 eV)   π$_{H-1}$ (-7.60 eV)   π$_H$ (-7.58 eV)   π$_L^*$ (-2.51 eV)

Figure S2. Frontier orbitals at the GS, PICT, and TICT minima of roseolumiflavin in the gas phase. MOs are computed at the BHLYP/TZVP level and visualized with MOLDEN using a contour value of 0.03. The MO energies are given in parentheses.

Ground State (GS)

n_{H-4} (-9.67 eV)

n_{H-3} (-9.44 eV) π_{H-1} (-7.79 eV) π_H (-7.00 eV) π_L^* (-2.01 eV)

Planar ICT (PICT)

n_{H-3} (-9.47 eV) π_{H-1} (-7.76 eV) π_H (-6.81 eV) π_L^* (-2.15 eV)

Perpendicular-Twisted ICT (TICT)

n_{H-3} (-9.57 eV) π_{H-1} (-7.59 eV) π_H (-7.07 eV) π_L^* (-2.52eV)

Figure S3. Frontier orbitals at the GS, PICT, and TICT minima of roseolumiflavin in water. MOs are computed at the BHLYP/TZVP level using the COSMO solvation model. They are visualized with MOLDEN using a contour value of 0.03. The MO energies are given in parentheses.

Ground State (GS)

n_{H-4} (-9.32 eV)

n_{H-3} (-9.30 eV)

π_{H-1} (-7.97 eV)

π_H (-7.17 eV)

π_L^* (-1.99 eV)

Planar ICT (PICT)

n_{H-3} (-8.93 eV)

π_{H-1} (-7.95 eV)

π_H (-7.07 eV)

π_L^* (-2.26 eV)

Perpendicular-Twisted ICT (TICT)

n_{H-3} (-9.26 eV)

HOMO-1 (-7.57 eV)

HOMO (-7.42 eV)

LUMO (-2.52 eV)

Figure S4. Frontier orbitals at the GS, PICT, and TICT minima of roseolumiflavin in benzene. MOs are computed at the BHLYP/TZVP level using the COSMO solvation model. They are visualized with MOLDEN using a contour value of 0.03. The MO energies are given in parentheses.

(a)	(b)

Figure S5. Kohn-Sham HOMO computed at the BHLYP/SVP level for the following model systems: (a) isolated RoLF; (b) RoLF in a micro-solvation shell of four water molecules. The plots were created with MOLDEN using an isosurface contour value of 0.02.
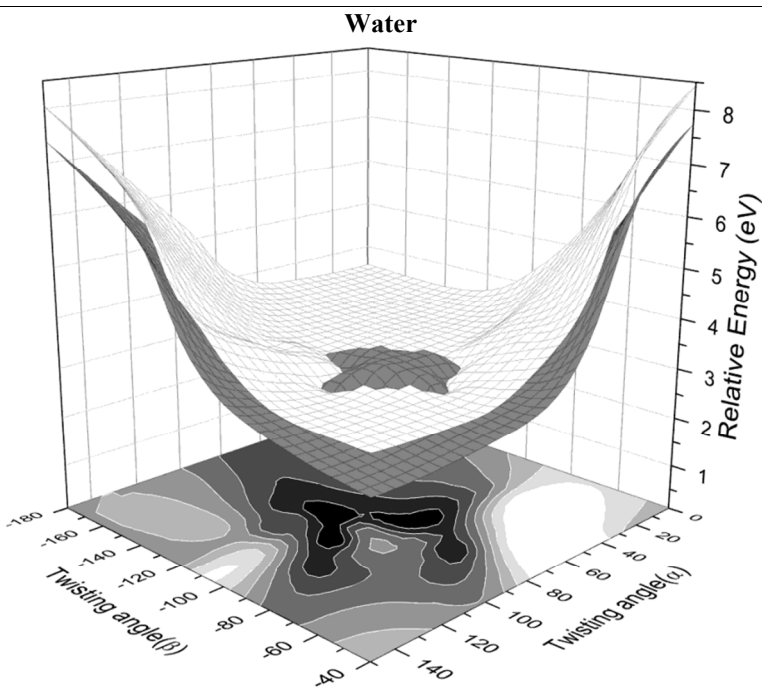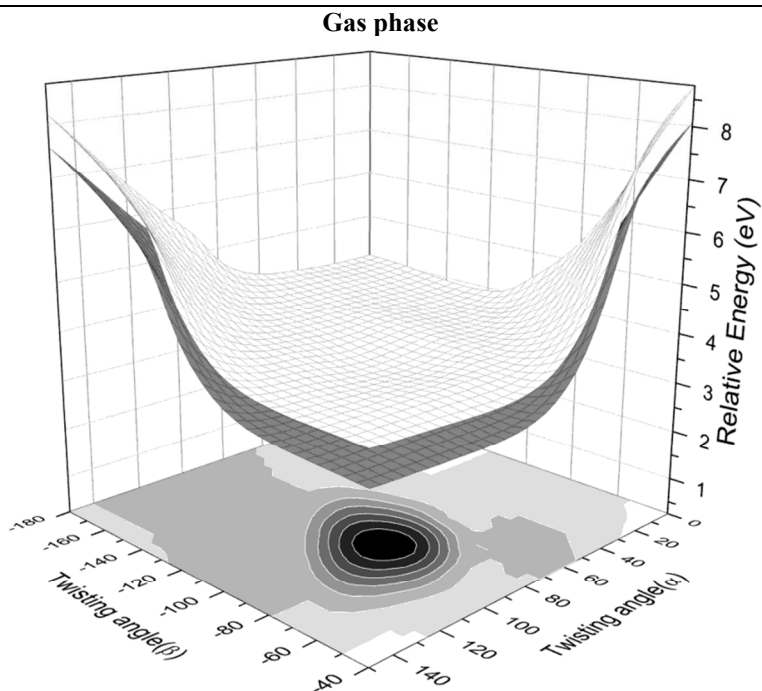
Gas phase

Water

Figure S6. 3D representation of the energy surfaces of the LE state (gray) and CT state (white) with respect to the dihedral angles (α and β, see Figure 2) related to the twist of the DMA group, as calculated in the gas phase (top) and in water (bottom) at the CAM-B3LYP/6-31G(d) level. Energies are given in eV relative to the GS minimum at the same level. The absolute values of

the energy difference between the LE and CT states at a given pair of α and β is presented as a black-and-white contour map at the bottom, where darker color corresponds to a lower energy difference. The quantitative picture of the LE-CT energy difference values can be found in Figure 7 of the main paper.

The absolute energy difference value of the two states for each dihedral pair is also depicted in Figure S6 as a 2D color map that is located at the xy-plane on the origin. This is essentially the same contour map as in the bottom panel of Figure 7, but in the latter, the absolute values of the energy differences are presented.
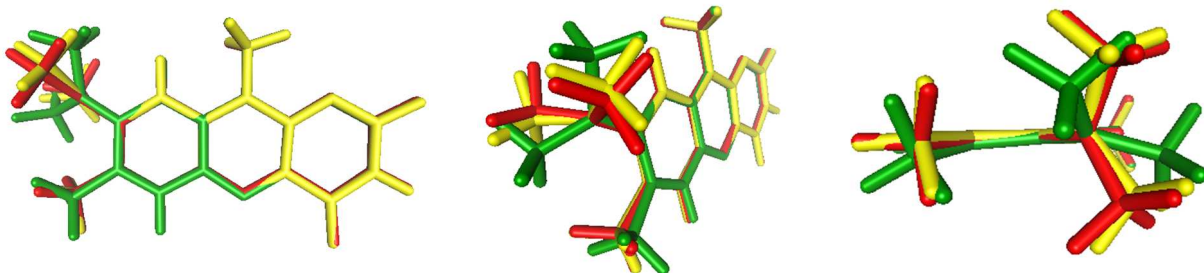
Figure S7. Superimposed stick representations of the minimum geometries of LE (green) and CT (red) states and of the conical intersection (CIn) of these states predicted at the DFT/MRCI level (yellow).

Vacuum	Water

Benzene	Micro-Solvation
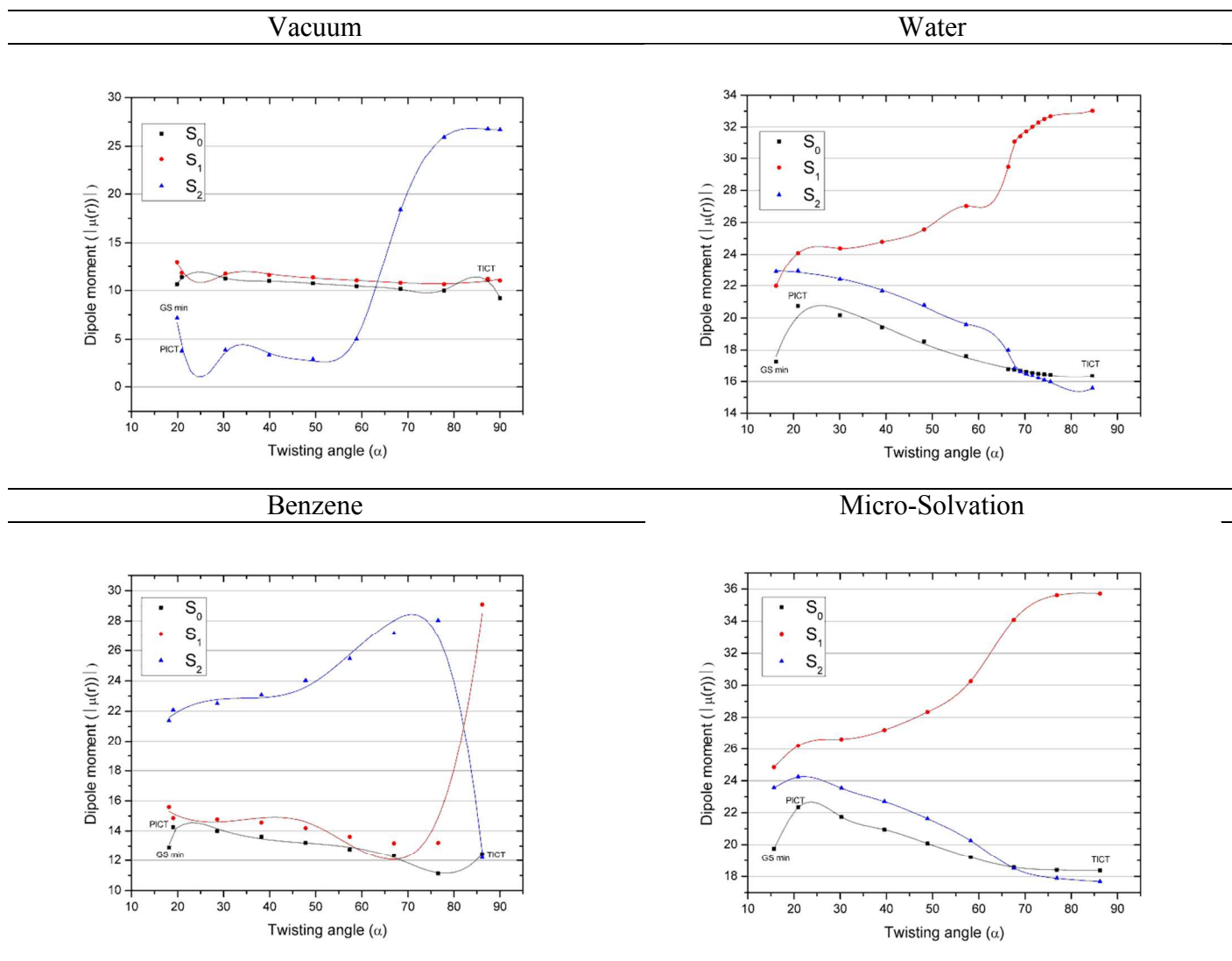
Figure S8. Magnitude of the dipole moment $|\mu(r)|$ (in Debye) in the ground state and low-lying singlet excited states as a function of the twisting angle (α, in degrees) computed at the DFT/MRCI level at the relaxed linear-interpolation geometries, as explained in Section 3.4.

In Figure S8, the states are denoted as S0, S1, and S2 instead of GS, LE, and CT (as in other figures) to underline that the adiabatic representation is used for the dipole moments, as opposed to the diabatic representation used for the energy values (based on the oscillator strength). This allows examination of the qualitative changes in the LE-CT character of the S1 and S2 states upon the twist of the DMA group.

D. Choice of micro-solvation model

Apart from the micro-solvation model described in the main paper (Figure 5) we considered two alternatives with one extra water molecule placed either next to the DMA substituent (model A) or next to the N1 atom in hydrogen-bonding distance (model B), see Figure S9.

The use of model A significantly affected the DFT/MRCI vertical transition energies, oscillator strengths, and dipole moments computed at the corresponding GS minimum (Table S7). This can be related to electron transfer in the HOMO from the DMA group to the added water (Figure S9). The "forced" interaction with the hydrophobic part of the DMA group of roseoflavin leads to an adverse effect, namely a hypsochromic shift of the first absorption peak (433nm) further away from the experimental value (503 nm). Moreover, the DFT/MRCI energies at the TICT minimum give the same order of the LE and CT states as at the GS minimum, because of a destabilization of the CT state (data not shown). This implies that the LE and CT surfaces do not cross, and hence there should be no ICT, contrary to experiments that assert the presence of an ICT for RoF in water.[3] Hence, model A with an extra water molecule near the hydrophobic DMA region of RoF is not realistic.

By contrast, the use of model B has only minor effects on the computed DFT/MRCI results. As evident from Table S7, the LE and CT energies relative to the corresponding GS energy change only very slightly (by 0.01 eV and 0.03 eV), and the same applies to the oscillator strengths and dipole moments. Likewise, the electron distribution in the HOMO remains rather unperturbed by the addition of an extra water molecule next to N1 (see Figure S9, original vs. model B).

Table S7. COSMO-corrected DFT/MRCI vertical excitation energies, oscillator strengths, and dipole moments of the singlet LE and CT states of RoLF in different micro-solvation models. The ground-state geometries were optimized at the CAM-B3LYP-level in water (CPCM).

Geometry Optimization Method	DFT/MRCI details	State	ΔE [eV]	λ [nm]	f(r)	$\|\mu(r)\|$ [Debye]
RoLF + 4 water (original)[a] CPCM (Water) + CAM-B3LYP	COSMO (Water, ε =78) [a]	LE	2.68	463	0.78	24.85
		CT	3.12	397	0.01	23.55
RoLF + 5 water (model A) CPCM (Water) + CAM-B3LYP	COSMO (Water, ε =78)	LE	2.86	433	0.53	18.87
		CT	3.29	377	0.16	26.00
RoLF + 5 water (model B) CPCM (Water) + CAM-B3LYP	COSMO (Water, ε =78)	LE	2.67	465	0.78	24.81
		CT	3.15	394	0.01	22.41
	Experimental (water)[b]	LE	2.47	503	0.48	
		CT				

[a] Also used in the main text (see Table 4).

Original	Model A	Model B
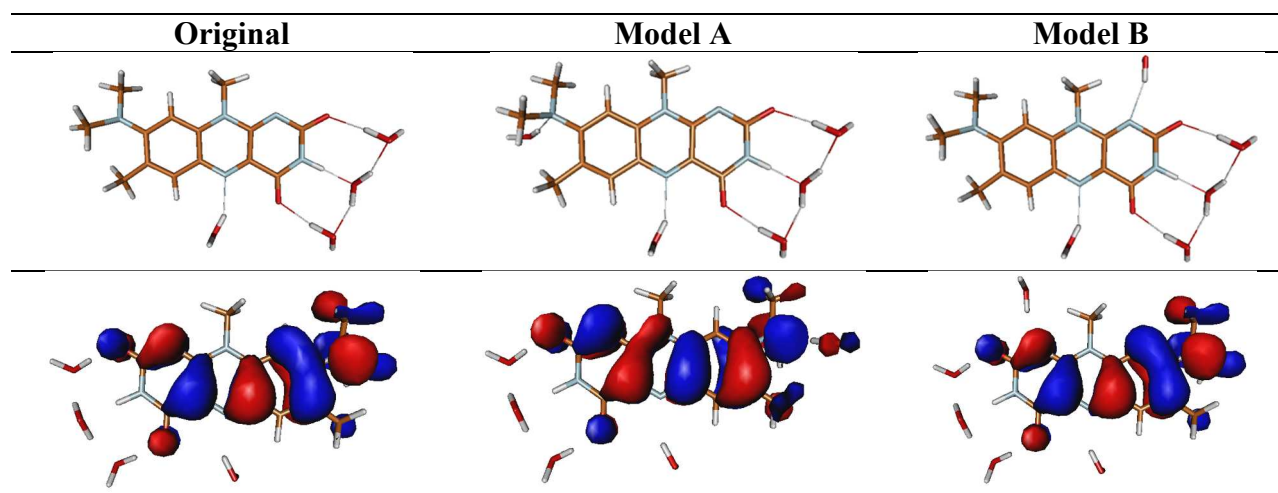
Figure S9. (Top) Stick representation of the three mico-solvation models considered here. (Bottom) Kohn-Sham HOMOs at the BHLYP/SVP level in the CPCM/water environment, computed at the ground-state minimum at the same level. "Original" denotes the model used in the main paper.

References:

(1) Yanai, T.; Tew, D. P.; Handy, N. C. *Chem. Phys. Lett.* **2004**, *393*, 51–57.

(2) Serganov, A.; Huang, L.; Patel, D. J. *Nature* **2009**, *458*, 233–237.

(3) Zirak, P.; Penzkofer, A.; Mathes, T.; Hegemann, P. *Chem. Phys.* **2009**, *358*, 111–122.

E. Color maps of energy contour plots
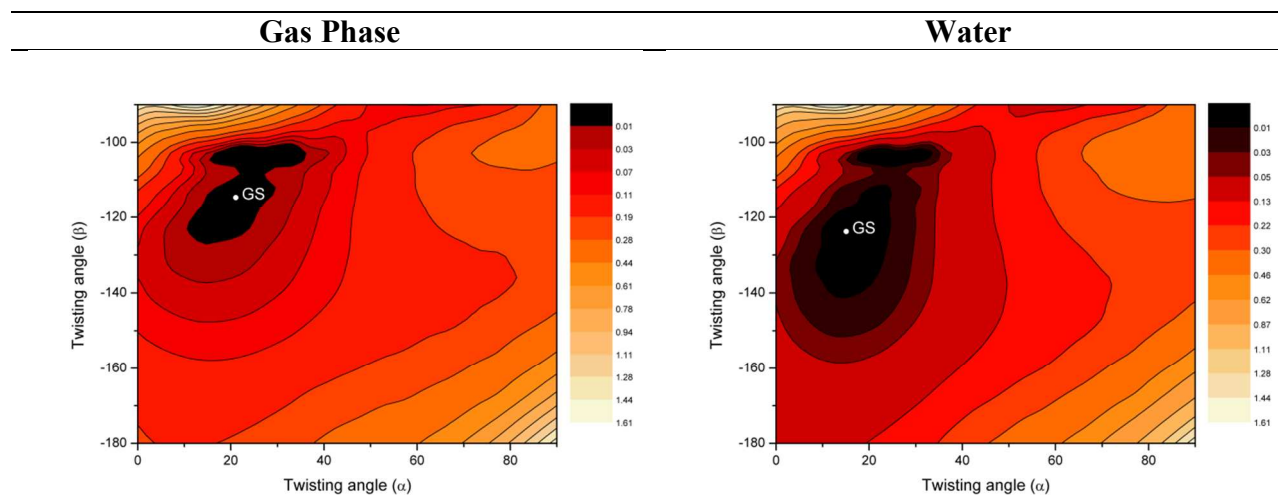
Gas Phase	Water

Figure S10. Energy color map (in eV) of 2D relaxed PES scans of the ground state with respect to the dihedral angles (α and β) in (a) the gas phase and (b) water. The white points with the label "GS" label indicate the position of the α/β pairs for the fully optimized stationary points.

	In vacuum	In water
LE Surface		
CT Surface		
ΔE(CT-LE)		
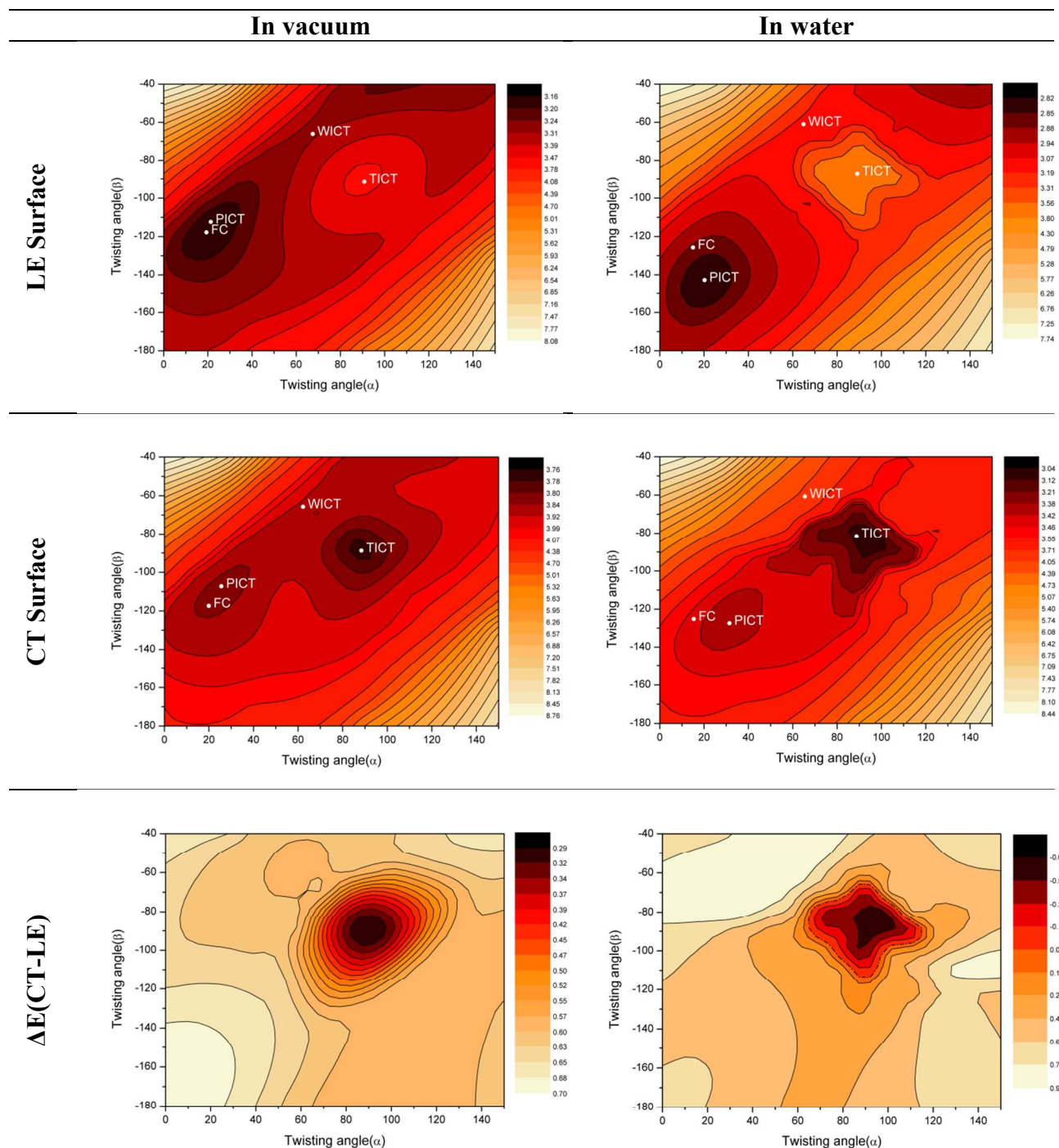
Figure S11. Energy color map (in eV) of 2D relaxed PES scans of the (top panel) LE and (middle panel) CT states with respect to the dihedral angles (α and β, see Figure 2). Bottom panel: Energy difference of the LE and CT states. The α/β pairs for the fully optimized stationary points for the PICT, TICT, and WICT species on the LE and CT surfaces and the projections of

the Franck-Condon point on each surface are indicated by white points with corresponding labels. Geometries were obtained at the CAM-B3LYP/6-31G(d) level in the gas phase (left column) and with CPCM corrections in water (right column) by following LE or CT state gradients. In the water case, the interpolated conical intersection seam is shown as dash-dot line; there is no such seam in the gas phase.